

# Network Pharmacology Experiments Show That Emodin Can Exert a Protective Effect on MCAO Rats by Regulating Hif-1 $\alpha$ /VEGF-A Signaling

Baojiang Lv,<sup>¶</sup> Kenan Zheng,<sup>¶</sup> Yifan Sun, Lulu Wu, Lijun Qiao, Zhibing Wu, Yuanqi Zhao,\* and Zequan Zheng\*



Cite This: *ACS Omega* 2022, 7, 22577–22593



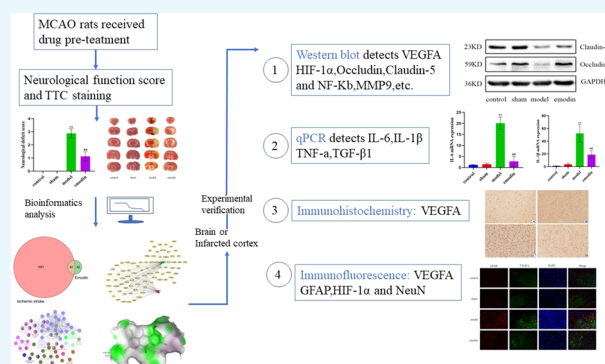
Read Online

ACCESS |

Metrics & More

Article Recommendations

**ABSTRACT:** Modern pharmacological studies have shown that emodin, the main effective component of rhubarb, has good anti-inflammatory and antioxidant effects, but its pharmacodynamic mechanism remains unclear yet. This study aims to elucidate the multitarget action mechanism of emodin in ischemic stroke through network pharmacology and *in vivo* experiments. Sprague–Dawley rats were randomly divided into control (normal saline), sham (normal saline), model (normal saline), and emodin groups ( $n = 9$  per group). Emodin was administered at 40 mg/kg/d for 3 consecutive days. The rats were subjected to middle cerebral artery occlusion for 2 h, followed by reperfusion for 24 h to establish the cerebral ischemia–reperfusion injury. To search for relevant studies in databases, emodin, ischemic stroke, and stroke were used as keywords. Subsequently, protein–protein interaction networks and complex disease target networks were established, and an enrichment analysis and molecular docking of core targets were performed. Gene expression was detected through western blotting and reverse-transcription polymerase chain reaction. Localization and expression of proteins were detected through immunohistochemistry. Furthermore, the neurological function, 2,3,5-triphenyltetrazolium chloride staining, levels of brain tissue inflammatory factors, the role of the blood–brain barrier (BBB), and relevant signaling pathways were assessed *in vivo*. The molecular docking of core targets revealed that the docking between vascular endothelial growth factor A (VEGF-A) and emodin was the most efficient. Emodin pretreatment decreased the neurological score from 2.875 to 1.125. Moreover, emodin inhibited the degradation of occludin and claudin-5 caused by matrix metalloproteinase (MMP)-2/MMP-9, thereby protecting the BBB. Additionally, related proteins such as hypoxia-inducible factor-1 $\alpha$ /VEGF-A and nuclear factor kappa B were down-regulated. Thus, emodin may play a protective role during cerebral ischemia reperfusion through mediation of the Hif-1 $\alpha$ /VEGF-A signaling pathway to inhibit the expression of inflammatory factors.



## 1. INTRODUCTION

Ischemic stroke is a disease with high disability and mortality rates in middle-aged and elderly people. However, epidemiological surveys have shown that this disease is gradually occurring in younger individuals also.<sup>1</sup> Rapid initiation of vascular recanalization is crucial for the clinical treatment of ischemic stroke. However, secondary ischemia–reperfusion (I/R) injury after vascular recanalization is a major cause of cell necrosis in infarcted lesions. Its oxidative stress and inflammatory response directly lead to the destruction of the blood–brain barrier (BBB) and reinjury of neurons.<sup>2</sup> Studies have demonstrated that vascular endothelial growth factor (VEGF) expression is harmful in the early stages of acute stroke, particularly between 1 and 24 h after stroke onset.<sup>3,4</sup> VEGF can cause BBB destruction and vascular leakage, which in turn cause

edema, increased intracranial pressure, and neuroinflammation, thereby exacerbating the expansion of the infarct volume.<sup>5</sup>

Vascular intervention and thrombolytic therapy are still the most desirable options for rescuing ischemic penumbra. However, this treatment has some limitations because of the narrow treatment window and several contraindications.<sup>6</sup> In addition, an I/R injury is an inevitable outcome for almost all patients with ischemic stroke.<sup>7</sup> Therefore, I/R injury reduction

**Received:** March 29, 2022

**Accepted:** June 6, 2022

**Published:** June 16, 2022



is the main direction of drug development for ischemic stroke. Thus, various drugs with anti-inflammatory, antioxidant, and neurotrophic effects have been used for brain protection therapy after stroke.

Natural compounds and their derivatives have been used to treat various diseases, including autoimmune diseases and cancer.<sup>8–10</sup> Rhubarb is the rhizome of *Rheum palmatum L.*, *Rheum officinale Baill.*, or *Rheum tanguticum Maxim. ex Balf.*<sup>11</sup> *Rheum palmatum L.* is a valuable medicinal plant widely distributed in the alpine and desert regions of Asia and Europe. It has anti-inflammatory,<sup>12</sup> antiviral, antipyretic, antitumor, and other biological activities.<sup>13,14</sup> According to Chinese medicine textbooks published by the Ministry of Education of China, most ischemic stroke types can be classified as heat syndromes, such as a decrease in qi and blood and an increase in wind and fire. Therefore, traditional Chinese medicines that reduce excess heat and purify fire are often used to treat ischemic stroke, such as *R. palmatum L.* Emodin is one of the main bioactive compounds extracted from the rhizome of *R. palmatum L.* Emodin has been proven to have protective effect on BBB and reduce the damage caused by I/R to stroke through multiple pathways such as antioxidant, anti-inflammatory, anti-proliferation, and anti-apoptosis.<sup>15–17</sup> Therefore, we conducted animal experiments and observed that emodin treatment can improve the clinical symptoms of middle cerebral artery occlusion (MCAO) in rats within 24 h and reduce the infarct volume. The results are consistent with those of previous studies.

To further explore the molecular action mechanism of emodin in ischemic stroke treatment, we used network pharmacology to predict the target gene and found that VEGF-A is the most critical drug target. A literature review revealed that emodin mainly inhibits VEGF-A, which can limit microvascular proliferation, reduce vascular leakage, and relieve inflammation.<sup>18</sup> However, whether emodin exerts an inhibitory effect on brain-derived VEGF-A is unknown. Furthermore, whether it improves MCAO by targeting and regulating VEGF-A function is unknown. These knowledge gaps must be filled with further studies. VEGF-A has a multifaceted regulatory role in the onset and prognosis of ischemic stroke, and studies have revealed that 24 h after stroke onset is a critical time for VEGF-A to exert its effects. Therefore, our study investigated the effect of emodin pretreatment within 24 h of MCAO to explore the effect of emodin on MCAO from the perspective of vascular proliferation and inflammation, which supplements the previous research gap on the action mechanism of emodin in ischemic stroke treatment.

Network pharmacology emphasizes systematicness, which coincides with the characteristics of traditional Chinese medicine. This study is the first to explore the action mechanism of emodin in the treatment of ischemic stroke by using network pharmacology combined with molecular docking and animal experiments. It is hoped that the research results provide an experimental reference for ischemic stroke treatment with traditional Chinese medicine.

## 2. MATERIALS AND METHODS

**2.1. Materials and Reagents.** The following materials and reagents were used in the study: Emodin (no.: A0044, Chengdu Must Biotechnology Co., Ltd., China, purity $\geq$ 98%); anti-MMP9 (no.: Ab38898, Abcam, U.K.); anti-NF- $\kappa$ B p65 (no.: #8242, CST, USA); anti-IKK $\beta$  (no.: #2678, CST, USA); 2,3,5-triphenyl tetrazolium chloride (no.: T8877-25G, Sigma, USA); hematoxylin and eosin (HE) staining kit (no.:BP-DL017,

SenBeijia Biological Technology Co., Ltd. China); HRP-labeled goat anti-rabbit IgG (H + L) (no.: A0208, Beyotime Biotechnology, China); anti-MMP2 (no.: Ab181286), anti-occludin (no.: Ab216327), anti-extracellular signal-regulated kinase [ERK1/2 (no.: Ab184699)], and p-anti-ERK1/2 (no.: Ab214036)—Abcam, U.K.; IL-6 antibody (no.: DF6087), HIF1A antibody (no./AF1009), claudin-5 (no./AF5216), and VEGFA antibody (no.: DF7470)—Affinity, China; Alexa Fluor 555-labeled donkey anti-mouse IgG(H + L) (A0460), Triton X-100 (no.: ST795), and antifade mounting medium (no.: P0126)—Beyotime Biotechnology, China; neutral balsam (no.: G8590, Beijing Solarbio Science & Technology Co., Ltd. China); RNA Easy Fast Tissue/Cell Kit (no.: DP451), FastKing gDNA Dispelling RT SuperMix (no.: KR118), and Talent qPCR PreMix (SYBR Green) (no.: FP209)—Tiangen Biotech (Beijing) Co., Ltd, China; anti-GAPDH (no.: AF7021, Affinity); and BCA Protein Assay Kit (no.: P0012S, Beyotime Biotechnology, China).

**2.2. Collection of Prediction Targets of Emodin.** We used the SwissTargetPrediction (<http://www.swisstargetprediction.ch/>),<sup>19</sup> Encyclopedia of Traditional Chinese Medicine (ETCM) (<http://www.tcmip.cn/ETCM/index.php/Home/Index/index.html>),<sup>20</sup> STITCH (<http://stitch.embl.de/>), and TargetNet databases (<http://targetnet.scbdd.com/>) as target search tools.<sup>21</sup> We used a set probability of  $\geq 0.10$  in the SwissTargetPrediction database and selected “*Homo sapiens*” from the options provided in the section “Choose an organism”. MedChemStudio software was used for target prediction in the ETCM database. According to the Chinese medicine ingredients used, after screening with MedChemStudio, this threshold value (high structural similarity, Tanimoto  $> 0.8$ ) was obtained as the predicted target. Furthermore, “0.40” was selected in the section “minimum required interaction score” in STITCH. Set probability selected was  $\geq 0.10$  in the TargetNet database. Emodin was used as the keyword to search for targets in each of the major databases. Simultaneously, the data retrieved from the literature were used as supplementary targets. The aforementioned retrieval projects were completed in October 2021. Genes obtained from databases and the literature were deduplicated and merged. Finally, these genes were used as the final prediction targets of emodin for subsequent analyses.

**2.3. Putative Targets of Ischemic Stroke.** The DisGeNET (<https://www.disgenet.org/>)<sup>22</sup> and GeneCards (<https://www.genecards.org/>)<sup>23</sup> databases were searched with “Ischemic stroke” and “cerebral infarction” as the keywords to identify ischemic stroke targets, and repeated targets were eliminated.

**2.4. Gene Name Correction and Target Screening.** UniProt database (<http://www.uniprot.org>) is the most informative and resourceful protein database. The data mainly come from protein sequences obtained after the completion of genome sequencing project and contain a lot of information about the biological function of proteins from the literature. UniProt database was used to standardize gene names for emodin and ischemic stroke. A Venny2.1.0 tool (<http://bioinfogp.cnb.sic.es/tools/venny/index.html>) was used to collect the common targets of the emodin and ischemic stroke.

**2.5. Network Construction and Core Target Screening.** The common targets were entered into the String database, where the organism was set as “*Homo sapiens*” to construct a protein–protein interaction (PPI) network; a medium confidence score  $> 0.4$  was selected. Then, the data obtained from the String database were input into Cytoscape v3.8.2 to visualize

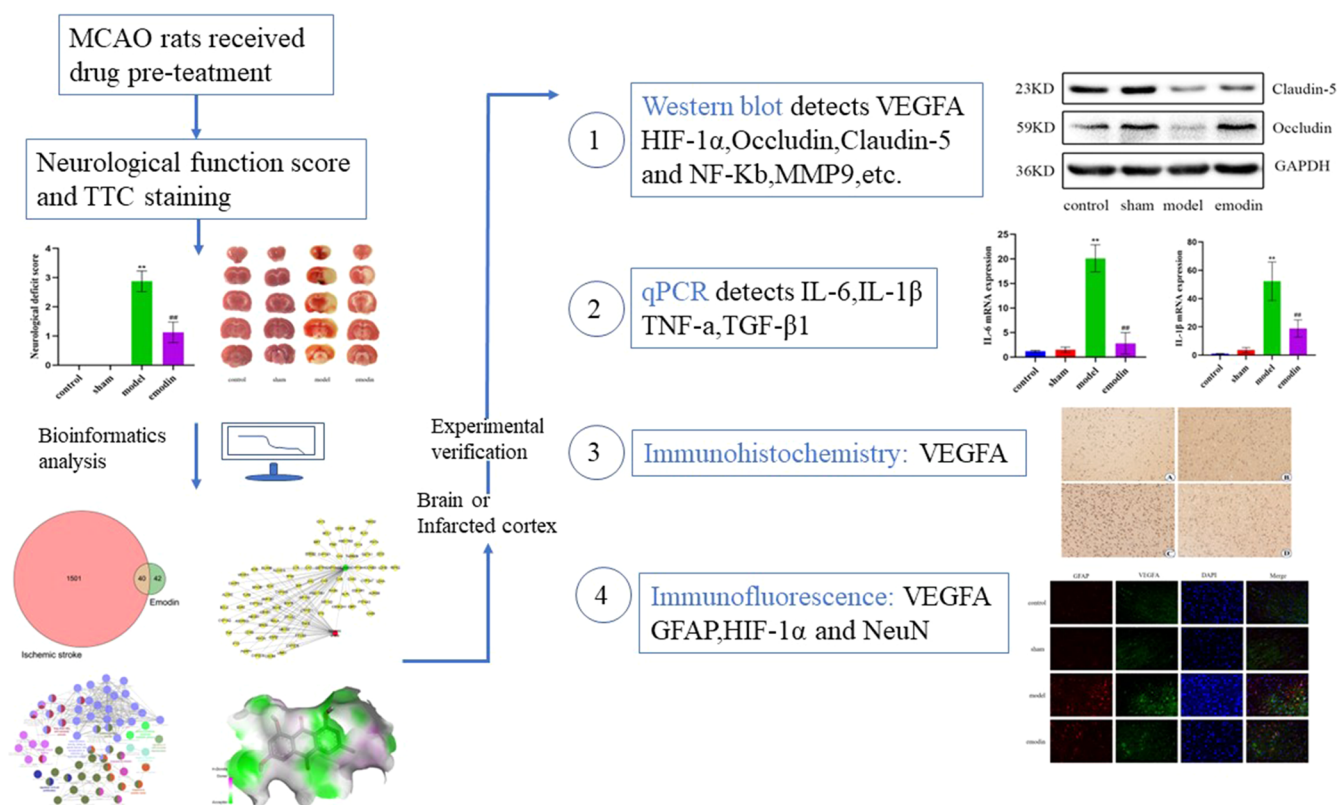


**Figure 1.** Scheme of the experimental procedure.

the PPI network. The PPI network was analyzed by Cytoscape plug-in cytoHubba to screen the core targets. A compound–target–disease network was constructed with utilization of Cytoscape 3.8.2 software. Modular clustering of the protein network was conducted to obtain core proteins with higher degrees by using the MCODE plug-ins in Cytoscape.

**2.6. Function and Pathway Enrichment Analysis.** Cytoscape’s ClueGO plug-in was used for enrichment analysis of Gene Ontology (GO) and Kyoto Encyclopedia of Genes and Genomes (KEGG). Three types of GO enrichment analyses were performed: biological process (BP), molecular function (MF), and cellular components (CC). The ClueGO plug-in was used to analyze the relationship between annotations and functional groups in biological networks to drill down into critical networks. In the ClueGO operation interface, the duplicate node was deleted. Species were restricted to *Homo sapiens*.  $P < 0.05$  was used as the screening target gene to analyze the main signal pathway and BP of emodin’s pharmacological action. Finally, the target-KEGG signal pathway-GO/BP network was constructed.

**2.7. Molecular Docking.** The interaction between the emodin and key targets was further verified by molecular docking, which provided a sufficient basis for emodin to treat ischemic stroke. Briefly, the SDF files of the three-dimensional chemical structures of emodin were downloaded from the PubChem database, and the three-dimensional chemical structures were optimized using ChemBio3D software. The structure of the target protein was obtained from protein data bank (PDB) database (<http://www.rcsb.org/>), and the complex was imported into AutoDockVina software for molecular structure processing and molecular docking. Discovery Studio software (Version 4.5) was used to analyze and visualize the binding mode and interactions of emodin and key target

proteins. The level of binding free energy was used as the evaluation standard of the binding degree of compounds. In general, the more stable the conformation of the compound molecule bound to the receptor, the lower the energy and the more reliable the result.

**2.8. Model Establishment and Grouping.** Thirty-six SPF Sprague–Dawley (SD) rats, weighing  $250 \pm 30$  g (3 months old, male), were purchased from the Experimental Animal Center of Southern Medical University [license number: SYXX(YUE)-2018-0094]. The experimental animals were raised in the Experimental Animal Center of Guangzhou University of Chinese Medicine at a temperature of  $24 \pm 2$  °C, humidity of 50–60%, free access to food and water, and 12 h light/dark cycle. After 1 week of adaptive feeding, the rats were anesthetized with pentobarbital sodium (30 mg/kg) and fixed on the operating table. The method of model construction was optimized by the consulting literature.

The right common carotid artery (CCA), external carotid artery (ECA), and internal carotid artery (ICA) were separated by blunt dissection of the skin layer by layer along the midline of the neck. During the operation, the accompanying nerve should not be damaged. The distal and proximal extremities of the external carotid arteries were ligated and then clipped. The ICA and CCA were clamped by vascular forceps, and the free end of the ECA was stretched to a straight line with the ICA. The free end of the ECA was pulled into a straight line with the ICA, then a small incision was opened at the free end of the ECA and the embolus was inserted. We extended along the label of the ICA close to the embolus and stopped insertion when there was significant resistance. At this point, the embolus reaches the anterior cerebral artery and blocks the middle cerebral artery. After 2 h of ischemia, the embolus was removed and the ECA wound was ligated. The rats were reperused for 24 h. The rats in

the sham group separated only the internal and external carotid arteries without blocking the middle cerebral artery. Other operations were the same as those in the model group. During the whole process, the room temperature was kept at  $25 \pm 0.5$  °C. At the same time, the temperature of rats was maintained at  $37 \pm 0.5$  °C with an electric pad. Local wounds were treated with penicillin to prevent infection before wound suturing.

Rhubarb is recognized as the plant *Rheum palmatum* L. in the polygonaceae family and has been checked on the websites [www.worldfloraonline.org](http://www.worldfloraonline.org) (World Flora Online) and [www.ipni.org](http://www.ipni.org) (International Plant Name Index). Emodin (batch number: A0044) was purchased from Chengdu Must Biotechnology Co., Ltd. (Chengdu, China), and the purity of emodin was  $\geq 98\%$ . The chemical structure of emodin is shown in Figure 2a.

SD rats were randomly divided into control group, sham group, model group, and emodin group, with nine rats in each group. The model group and emodin group were established by the above methods. Three days before operation, rats in emodin group were pre-treated with emodin (40 mg/kg/d). The dose of emodin was based on previous studies showing a neuro-protective effect in ischemic stroke. The other groups were given the same amount of normal saline. Using this animal model, our lab produced consistent ischemic damage in rodent brains, as evidenced by cerebral infarction visualization and behavioral analysis. All experiments followed the principles of randomization and double blindness. The procedure of the experiment is presented in Figure 1.

**2.9. Statement of Animal Ethics.** Experimental animals and animal experiments were approved by the Ethics Committee of Experimental Animals of Guangdong Provincial Hospital of Traditional Chinese Medicine (no.: 2020080), in compliance with internationally recognized and institutional guidelines for the care and use of animals. All animal experiments in this study were conducted in strict accordance with the recommendations in the National Health Organization's (NIH) Guidelines for the care and use of laboratory animals. During the experiment, the rats were anesthetized to reduce pain and injury. The rats in poor condition were raised separately after modeling. The operation of the whole experiment was gentle, without strong noise, which can reduce the stress response of animals.

**2.10. Neurological Severity Score.** Behavior observation was performed 24 h after operation. According to the neurological severity score (NSS) scoring standard, the motor, sensory, reflex, and balance functions of each group were evaluated comprehensively. This score was based on Zea Longa's five-point system.<sup>24</sup> The details are as follows: 0: normal, no neurological deficit; 1, the left front paw cannot be fully extended, mild neurological deficit; 2, when walking, the rat turns to the left (paralyzed side) in a circle, moderate nerve functional impairment; 3, when walking, the rat's body falls to the left, severe neurological deficit; 4, unable to walk spontaneously, loss of consciousness. A score of 1–3 points was considered a successful model,<sup>25</sup> and these rats were included in the experimental group according to the treatment.

**2.11. Measurement of the Cerebral Infarction Volume.** TTC staining was used to determine the infarct volume of MCAO rats. The brain tissue was taken and frozen at  $-20$  °C for 20 min. The coronal plane was sectioned continuously with a thickness of 2 mm and the brain was cut into five slices. The sections were incubated in 2% TTC (triphenyltetrazolium chloride) solution at 37 °C in the dark for 15 min. The infarcted area is pale, and normal brain tissue is dark red. The percentage

of infarct volume to cerebral hemisphere volume on brain slices was calculated by using the Image-Pro Plus 6.0 software.

**2.12. Quantitative Reverse Transcription-PCR.** After 24 h of ischemia reperfusion, the rats were sacrificed, and the cortical infarcted part of the brain tissue was cut out. Total ribonucleic acid (RNA) was extracted using RNA Easy Fast Tissue/Cell Kit. The total RNA concentration and OD260/OD280 value were measured by a spectrophotometer. The reverse transcription procedure of total RNA was carried out strictly in accordance with the manufacturer's instructions. qRT (quantitative reverse transcription)-PCR was carried out using SYBR Green Talent qPCR PreMix under the following thermocycling conditions: 95 °C for 3 min and 40 cycles at 95 °C for 5 s and 60 °C for 32 s. PCR primers were designed for each gene according to the NCBI reference sequence database. The primers were designed online by Primer-BLAST in NCBI and synthesized by IGE Biology (Guangzhou IGE Biotechnology Ltd). The primer sequence is shown in Table 1.  $\beta$ -Actin was used as the internal control for PCR. The relative mRNA expression was calculated using the  $2^{-\Delta\Delta C_t}$  method.

**Table 1. PCR Primers**

gene	sequence
IL-1 $\beta$	F: 5'-TGAAATGCCACCTTTTGACAGTG-3' R: 5'-ATGTGCTGCTGCGGATTTG-3'
IL-6	F: 5'-AGCCAGAGTCCTTCAGAGAGA-3' R: 5'-GCCACTCCTTCTGTGACTCC-3'
TNF- $\alpha$	F: 5'-GGTGCCATGTCTCAGCCTCTT-3' R: 5'-GCCATAGAAGTATGAGAGGGAG-3'
TGF- $\beta$	F: 5'-AGGGCTACCATGCCAACTTC-3' R: 5'-CCACGTAGTAGACGATGGGC-3'
$\beta$ -actin	F: 5'-GCAGGAGTACGATGAGTCCG-3' R: 5'-GGGTGTAACGCAGCTCAG-3'

**2.13. Immunohistochemistry.** The paraffin sections of 5  $\mu$ m were dewaxed, and the brain sections were fixed in tris-EDTA/citrate buffer solution (10 mmol/L, pH 6.0) for microwave repair. The brain sections were incubated with 3% hydrogen peroxide for 30 min and rinsed with PBS. Goat serum was blocked for 10 min, rinsed with PBS, added with primary antibody (anti-VEGFA, 1:1000), and incubated overnight at 4 °C. After rewarming, PBS was rinsed, and secondary antibody was added and incubated at room temperature for 1 h. DAB solution was added for color development, and then, tap water was stopped for color development. Hematoxylin was redyed for 5 min, and 1% hydrochloric acid ethanol was used for differentiation. Gradient ethanol was used to dehydrate the slices, and neutral resin was used to seal the slices.

**2.14. Western Blot.** According to a previously established method,<sup>26</sup> RIPA and PMSF were prepared in a working solution that was used to extract the total protein of brain tissues. The protein concentration was determined by BCA method. The same amount of protein was loaded into SDS-PAGE gel for electrophoresis. The PVDF membranes with proteins were incubated with diluted primary antibodies at 4 °C overnight. The membranes were incubated with relative sources of secondary antibodies (1:2000) at room temperature for 1 h. Finally, proteins were visualized by chemiluminescence and quantitatively analyzed using ImageJ software.<sup>27</sup> Bands were normalized to GAPDH. The dilution ratio and brand of antibody are shown in Table 2.

**Table 2. Brand and Dilution Ratio of Each Antibody**

antibody name	dilution ratio	product code	brand
MMP-9	1:5000	ab76003	Abcam, UK
MMP-2	1:1000	ab181286	Abcam, UK
NF- $\kappa$ B p65	1:1000	#8242	CST, USA
IKK $\beta$	1:1000	#2678	CST, USA
occludin	1:1000	ab216327	Abcam, UK
ERK1/2	1:10000	ab184699	Abcam, UK
phospho -ERK1/2	1:1000	ab214036	Abcam, UK
IL6	1:2000	DF6087	Affinity, China
HIF1A	1:2000	AF1009	Affinity, China
VEGFA	1:2000	ab231260	Abcam, UK
claudin 5	1:2000	AF5216	Affinity, China

**2.15. Double Immunofluorescence Staining.** 24 h after reperfusion, the rats in each group were anesthetized by intraperitoneal injection of pentobarbital. Rats from the groups underwent transcatheter perfusion with saline and then 4% PFA. The brain samples were taken out rapidly and embedded in paraffin blocks using a paraffin embedding station and then sectionalized (5  $\mu$ m) using a rotary microtome. TritonX-100 PBS was incubated with 0.2% (volume fraction) for 10 min; then washed with PBS and blocked with 5% (volume fraction) goat serum at room temperature for 30 min; anti-Neun antibody (1:1000), glial fibrillary acidic protein (GFAP) mouse monoclonal antibody (1:100), VEGFA antibody (1:200), and anti-Hif-1 $\alpha$  antibody (1:500) were incubated overnight in a wet box at 4  $^{\circ}$ C; and the primary antibody was rinsed with PBS 5 times for 3 min and rotated dry. Donkey anti-rabbit IgG(H + L)-Z (1:100) and Donkey anti-mouse IgG(H + L)-Z (1:100) were incubated in a wet box at room temperature for 30 min in dark. DAPI was added, and the slides were incubated for 5 min in darkness. The slide was shaken to remove moisture, and the DAPI was washed with PBS solution. The anti-fluorescence quenching agent was dropped onto the slide, and the slide was sealed away from light. It was observed under an automatic inverted fluorescence microscope.

**2.16. Statistical Analysis.** SPSS 26.0 software (IBM Corp) was used for statistical analysis of the data, and all the data were represented by mean  $\pm$  standard deviation ( $\bar{x} \pm s$ ) for normality test, and difference between groups was tested by one-way analysis of variance (ANOVA);  $P < 0.05$  was considered to be statistically significant.

### 3. RESULTS

**3.1. Emodin Can Alleviate the Symptom of MCAO within 24 h and Reduce the Cerebral Infarct Volume.** In order to evaluate the effect of emodin on MCAO in 24 h, we observed the difference of clinical symptoms in each group by comparing m-NSS scores and the size of infarction by TTC staining. TTC staining of rat brain showed that normal brain tissue was red and infarcted brain tissue was white (Figure 2b). The results showed that the NSS score of the model group was significantly higher than that of the sham group ( $P < 0.01$ ). Compared with the model group, the symptoms of nerve injury were alleviated and the NSS scores significantly decreased in the emodin group ( $P < 0.01$ ), as shown in Figure 2c. The percentage of infarct area in emodin group was significantly lower than that in the model group ( $P < 0.01$ ), as shown in Figure 2d. These results indicated that emodin could alleviate the symptoms of MCAO rats in the acute phase and reduce the infarct volume.

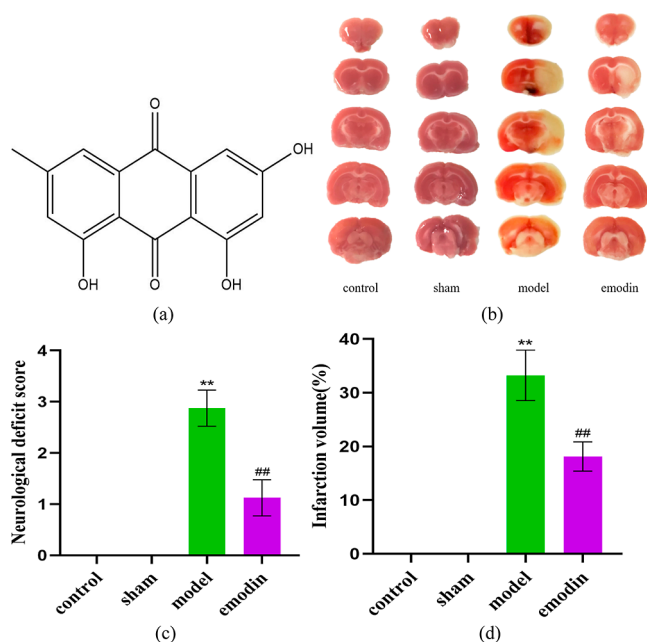


**Figure 2.** Effects of emodin on neurological function score and cerebral infarction volume in MCAO rats. (a) Structure of emodin. (b) TTC staining was used to observe the volume morphology of cerebral infarction. Infarcts appear white, while non-infarcts are red. (c) Effect of emodin on neurological deficit score in MCAO rats. (d) Effect of emodin on the infarction volume of brain tissue in MCAO rats. Data are presented as mean  $\pm$  SEM; \* $P < 0.05$ , \*\* $P < 0.01$  vs sham group; # $P < 0.05$ , ## $P < 0.01$  vs model group.

**3.2. Emodin Target Screening and Collection.** In order to explore the potential molecular mechanism of emodin in the treatment of ischemic stroke, we collected and screened the targets of emodin. Through the comparison and screening of multiple databases, the ADME parameters and related molecular weights of emodin were obtained: its molecular formula is  $C_{15}H_{10}O_5$ . The molecular weight is 270.2369 g/mol; the drug similarity grade is "good"; the CAS number is 518-82-1; the number of smiles is CC1=CC2=C(C(=C1)O)C(=O)C3=C(C2=O)C=C(C=C3O)O. The targets of emodin were retrieved from ETCM, SwissTargetPrediction, STITCH, and TargetNet databases, and 15, 38, 10, and 31 targets were obtained, respectively. After the repeated targets were deleted, a total of 82 targets were obtained, as shown in Table 3.

**3.3. Construction of Ischemic Stroke-Related Targets and Venn Diagrams.** According to the screening criteria, 5970 and 1159 genes related to ischemic stroke were searched from GeneCard and DisGeNET databases, respectively. After deduplication and conversion, a total of 1545 genes related to ischemic stroke were obtained. The ischemic stroke-related genes were mapped to emodin-related targets to obtain a total of 40 intersecting genes (Figure 3a), which were used as target genes for emodin against ischemic stroke. The target-disease network was constructed as shown in Figure 3b.

**3.4. PPI and Related Network Construction.** According to the screened emodin and disease-related genes, the compound–target–disease network was constructed as shown in Figure 3b. From the network, it could be seen that emodin can act on ischemic stroke through multiple target genes. The String software was used to generate the PPI network. The TSV file was imported into Cytoscape to construct the PPI network, as shown in Figure 4c. There were 39 nodes and 203 edges in the network.

Table 3. Summary of Emodin Targets Screened from Various Databases

ESR1	LIMK1	AURKB	AKR1B1	CYP1A2	NR1H2	TUBB2B	CES2
PIM1	LCK	KDR	CDK5R1	CYP2C9	NR1H3	RELA	CA7
ESR2	CYP19A1	PLK1	CCNB3	CYP2D6	TP53	CA5A	HSD17B1
CSNK2A1	ABCB1	MET	CDK6	CYP2E1	VEGFA	MAOB	RIPK2
PTP4A3	BCHE	AXL	ABCG2	CYP3A4	CASP3	CA14	CA13
ELANE	XDH	PARP1	CBR1	CYP3A43	ERBB2	MAOA	CASB
FNTA	ADORA3	TNKS2	LDHA	CYP3A5	TNF	PTGS1	CA4
MCL1	CYP1B1	TNKS	LDHB	CYP3A7	CXCR4	MIF	CA6
BCL2	FASN	CRHR1	AHR	GSTA1	PTGS2	ALOX15	ALPL
FTO	EGFR	DRD3	ALOX5	GSTP1	STS	CES1	TLR9
HSD17B2	CA9						

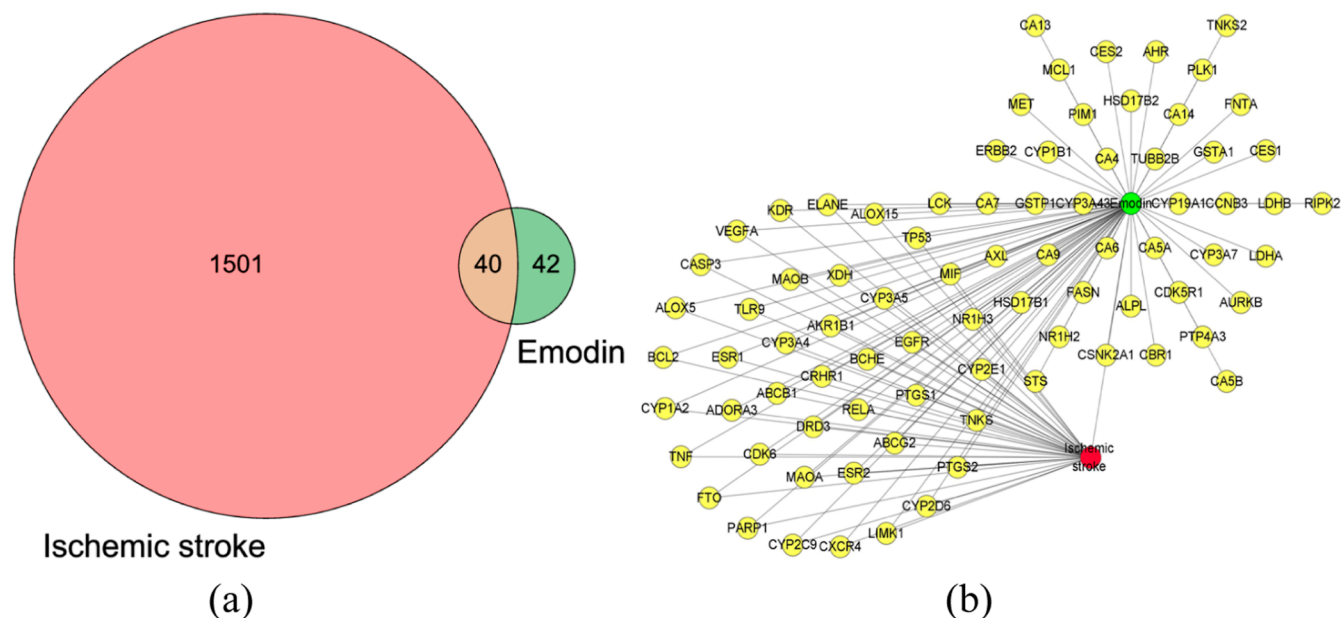


**Figure 3.** Emodin anti-ischemic stroke target and its interaction network. (a) Venn diagram of target intersection: the pink circle represents the ischemic stroke target, and the green circle represents the emodin target. There are 40 intersection targets between them; (b) emodin–target–disease network diagram: the yellow circle represents the target gene, red represents disease, and green represents emodin. There are 84 nodes and 123 edges in the network, and the average number of adjacent nodes is 2.929.

The average number of adjacent nodes was 10.410, and the clustering coefficient was 0.614. The scores of nodes were calculated by cytoHubba. VEGFA, tumor necrosis factor (TNF), CASP3, TP53, and PTGS2 were the top 5 targets. These genes are related to vascular endothelial formation, inflammation, apoptosis, and oxidation. The node represents the ingredient and its corresponding target. The higher the degree of the node, the greater the role of component or target in pharmacological course. There were 19 genes with degree greater than 10, as shown in Table 4.

PPI networks of emodin and ischemic stroke targets were constructed, respectively, as shown in Figure 4a,b. There are 1310 nodes and 7958 edges, 5465 nodes and 27645 edges in the network, respectively. The alluvial diagram of emodin signaling pathway in ischemic stroke is shown in Figure 4e. To analyze the relationship between emodin target and ischemic stroke, molecular complex detection (MCODE) uses a vertex weighted scheme to discover locally high-density regions in network graphs. It is widely used in all kinds of network analysis modules to expand the nodes as the center and to find the nodes that meet the requirements in the neighboring nodes. To further explore PPI network information, MCODE was used to calculate a total of 4 module networks, as shown in Figure 5. In module 1, TNF,

TLR9, ELANE, and CXCR4 are mainly related to inflammation and immunity, and genes such as AKR1B1, EGFR, and ABCB1 are related to regulate angiogenesis and apoptosis and promote BBB permeability; Module 2 has CYP3A5, CYP2E1, and CYP2D6 and other cytochrome oxidase-related genes, which may be involved in oxidative metabolism; Module 3 has VEGFA, TP53, MIF, and other genes, which may be involved in angiogenesis and cell proliferation; Module 4 is mainly related to human monoamine oxidase such as MAOA and MAOB and emotional consciousness. Finally, Cytoscape was used to construct the emodin–target–disease–GO/BP-KEGG pathway network, as shown in Figure 6. There are 114 nodes and 359 edges in the network. The results suggest that emodin may participate in the treatment of ischemic stroke through complex BPs and related signaling pathways.

**3.5. Enrichment Analysis.** The Cytoscape plug-in ClueGo was used for GO and KEGG enrichment analyses. According to the filtration conditions, GO-related items BP, CC, and MF were obtained, as shown in Figure 7a,b, and KEGG enrichment analysis is shown in Figure 7c,d. There were 41 KEGG and 93 GO terms in total, which met the requirements of count  $\geq 2$  and  $P$ -value  $< 0.05$ . Most targets are related to inflammatory response, angiogenesis, trauma response, positive regulation of

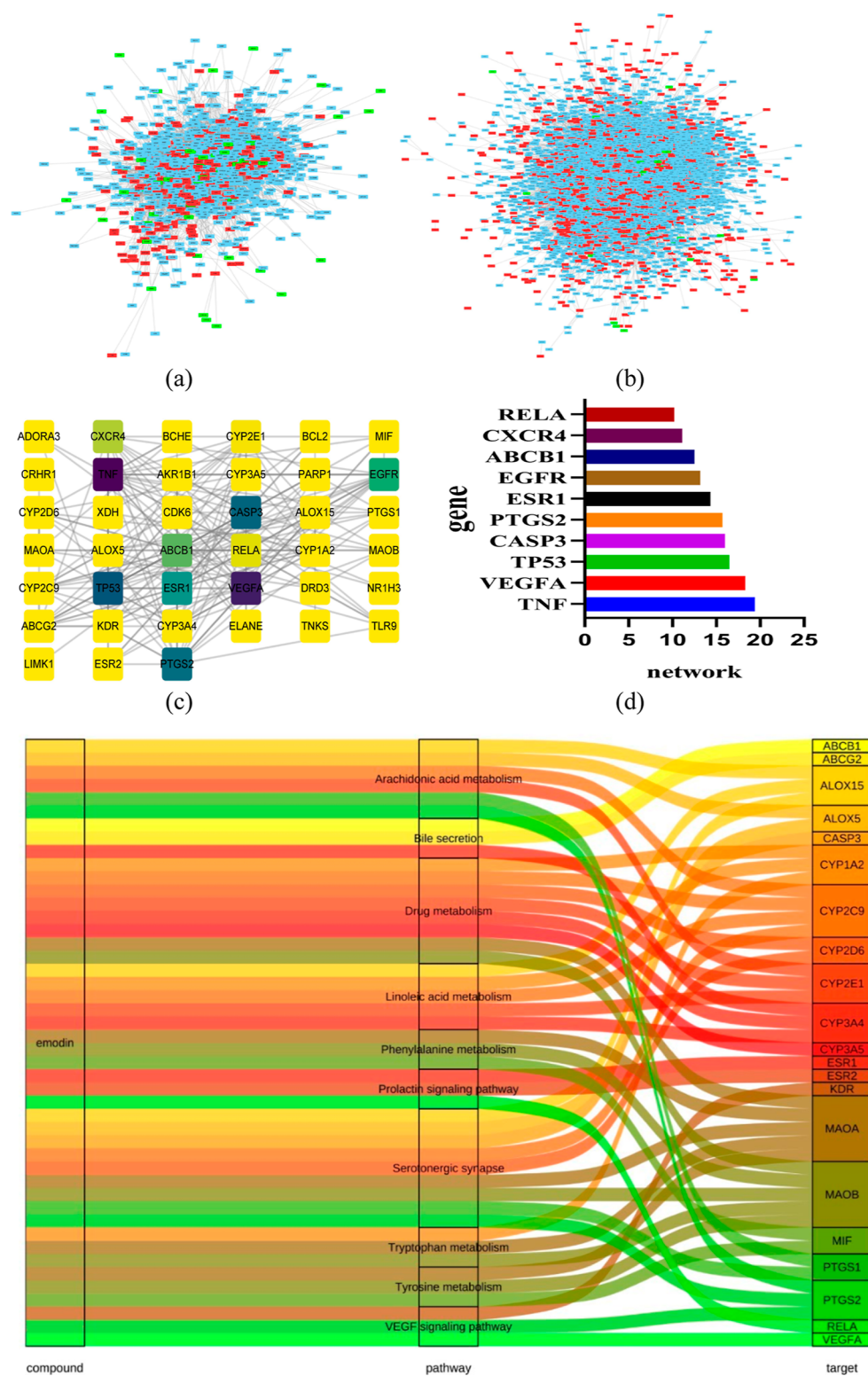


**Figure 4.** (a) PPI network of emodin targets. (b) PPI network of disease targets. The red and green dots represent the targets of ischemic stroke and emodin, respectively. (c,d) PPI network of intersection targets. The PPI network was constructed through the String website, and the top 10 core targets were obtained through the MCC algorithm of cytoHubba plug-in of Cytoscape. (e) Alluvial map of emodin signaling pathway in ischemic stroke.

multicellular BPs, oxygenated compound response, reactive oxygen metabolism process, and response to drugs. The top 5 GO terms are regulation of mitochondrial depolarization, phenol-containing compound metabolic process, catecholamine metabolic process, negative regulation of calcium ion transport,

and negative regulation of calcium ion transmembrane transporter activity. After KEGG enrichment analysis, 41 pathways were obtained. The relevant KEGG terms are VEGF signaling pathway, prolactin signaling pathway, bile secretion, arachidonic acid metabolism, and linoleic acid metabolism. Among them, the

Table 4. Top 20 Intersection Genes (Sorted by Degree Value)

uniprot ID	target protein	gene	closeness	degree
P15692	VEGF A	VEGFA	0.7169811	24
P01375	TNF	TNF	0.6666667	22
P42574	caspace-3	CASP3	0.6909091	22
P04637	cellular tumor antigen p53	TP53	0.6909091	22
P35354	prostaglandin G/H synthase 2	PTGS2	0.6333333	20
P03372	estrogen receptor	ESR1	0.6440678	18
P00533	epidermal growth factor receptor	EGFR	0.6333333	17
P08684	cytochrome P450 3A4	CYP3A4	0.6031746	16
P08183	ATP-dependent translocase ABCB1	ABCB1	0.6031746	16
P61073	C-X-C chemokine receptor type 4	CXCR4	0.61290324	15
Q9UNQ0	broad substrate specificity ATP-binding cassette transporter ABCG2	ABCG2	0.5846154	14
P05181	cytochrome P450 2 × 10 <sup>1</sup>	CYP2E1	0.5671642	13
Q04206	transcription factor p65	RELA	0.5588235	12
P11712	cytochrome P450 2C9	CYP2C9	0.5507246	12
P09917	polyunsaturated fatty acid 5-lipoxygenase	ALOX5	0.53521127	11
P05177	cytochrome P450 1A2	CYP1A2	0.5277778	11
P35968	VEGF receptor 2	KDR	0.5588235	11
P10635	cytochrome P450 2D6	CYP2D6	0.5205479	10
P15121	aldo-keto reductase family 1 member B1	AKR1B1	0.5205479	10
Q9NR96	toll-like receptor 9	TLR9	0.5135135	9

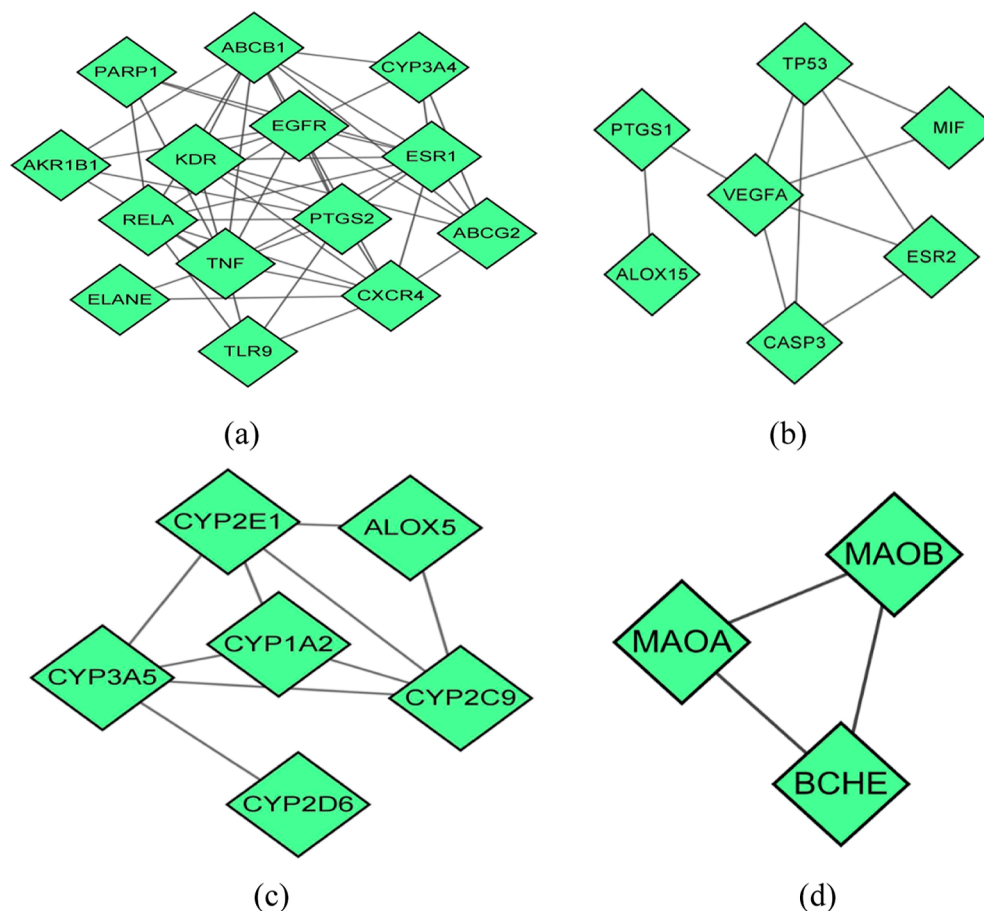


**Figure 5.** After PPI network is decomposed by MCODE, 4 clustering modules are obtained: (a–d) represent MCODE1, MCODE2, MCODE3, and MCODE4, respectively. Module 1 scored 8.154 points, with 14 nodes and 53 edges; Module 2 scored 4, with 6 nodes and 10 edges; Module 3 scored 3.667, with 7 nodes and 11 edges; and Module 4 scored 3. There are 3 nodes and 3 edges.

VEGF pathway was closely related to the vascular proliferation, oxidative stress, and inflammatory response secondary to ischemia and hypoxia.

**3.6. Molecular Docking Verification.** Based on the results of PPI and enrichment analysis, we believe that the first five targets may be more directly related to the anti-ischemic stroke effect of emodin. Therefore, this possible effect was verified by

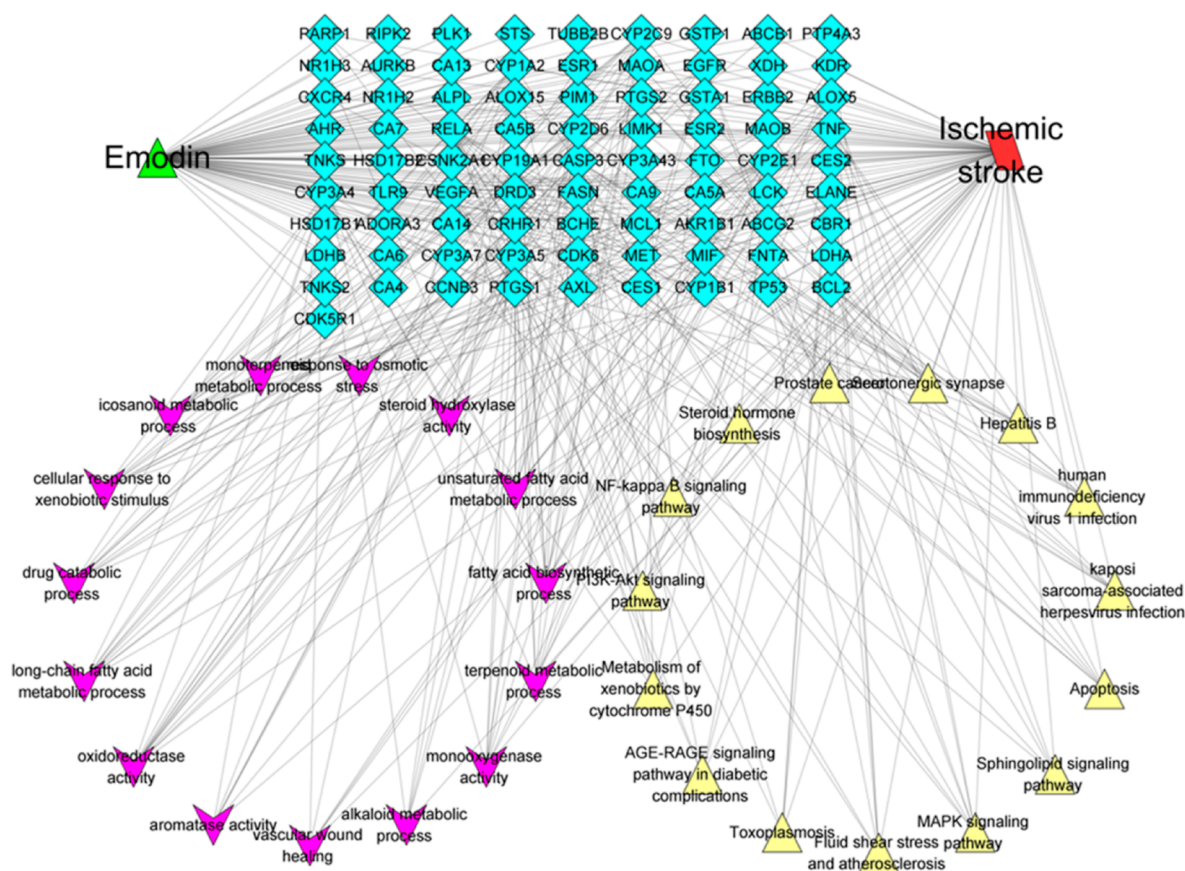


**Figure 6.** Emodin–target–disease–GO/BP–KEGG signaling pathway network diagram. The green triangle represents emodin, the blue diamond represents the target, the red quadrilateral represents ischemic stroke disease, the purple inverted triangle represents GO rich set of BPs, and the yellow triangle represents the KEGG pathway. There are 114 nodes and 359 edges in the network.

molecular docking. AutoDock software was used to analyze the core proteins (VEGFA, TNF, CASP3, TP53, and PTGS2) in the “component–target” network. Discovery Studio software was used to analyze the two-dimensional plan of molecular docking and the connection relationship between hydrogen bonds, as shown in Figure 8 (Figure 8 shows only the group with the best docking binding energy fraction, namely, emodin and VEGFA). The lower the fraction of binding energy, the more stable the binding between ligand and receptor. The results showed that the binding energies of emodin and core protein were less than  $-6$  kcal/mol, as shown in Table 5. Emodin formed hydrogen bonds with the amino acid residues His39, Gln461, Glu465, and Cys47 in VEGFA. According to the binding energy, we finally selected VEGFA as the target for the next step of molecular mechanism verification.

**3.7. Emodin Could Inhibit the Activation of VEGF-A in MCAO Rat within 24 h.** VEGF-A participates in a variety of pathogenic mechanisms after cerebral ischemia and reperfusion, including increasing vascular leakage and inducing a series of inflammatory reactions.<sup>5</sup> Based on the results of network pharmacology and molecular docking, we validated the mechanism of VEGF-A, which has the highest degree of enrichment degree and molecular binding. The immunohistochemistry results indicated that the intensity of VEGF-A in the brain of model rat was obviously enhanced than that of sham rat, indicating that VEGF-A was overexpressed in model rat. Emodin administration decreased VEGF-A staining intensity of MCAO rats (Figure 9a,b). What is more, western blotting (WB) results further showed that emodin reduced the level of VEGF-A

(Figure 9c,d) ( $P < 0.05$ ). These findings demonstrated that emodin down-regulated the level of VEGF-A, thereby protecting BBB and reducing vascular leakage of mcao rat.

**3.8. Emodin May Have a Protective Effect on the BBB in MCAO Rats.** Previous studies have shown that VEGF-A can cause hypoxia-induced vascular leakage and activation of matrix metalloproteinase, leading to BBB dysfunction.<sup>3,28,29</sup> Here, we detected the tight junction proteins occludin and claudin-5 and matrix metalloproteinase MMP-2/MMP-9 of the infarct lesion. The relative quantitative result of the two tight junction protein is shown in Figure 10a,c. The levels of tight junction proteins (occludin, claudin-5) and inflammation marker proteins (MMP-2, MMP-9) were determined to further investigate the effects of emodin on tight junction and inflammation. WB results show that treatment with emodin can up-regulate the levels of occludin and claudin-5 and down-regulate the levels of MMP-2 and MMP-9 in the infarcted cortex to different degrees (Figure 10). This indicates that emodin could inhibit the production of MMP-2/MMP-9, reduce the degradation of tight junction protein, and protect the permeability of BBB, thereby reducing the double damage of inflammation to brain tissue.

**3.9. Emodin May Reduce the Transcription of Inflammatory Factors through the ERK/IKK $\beta$ /NF- $\kappa$ B Signal.** Vascular leakage, inflammation, and cell proliferation caused by VEGF are mainly mediated *via* the ERK/IKK $\beta$ /NF- $\kappa$ B signal,<sup>5,30</sup> so we used WB and qRT-PCR to detect the expression of the signal protein and the mRNA transcription level of cytokines. The qRT-PCR results are shown in Figure



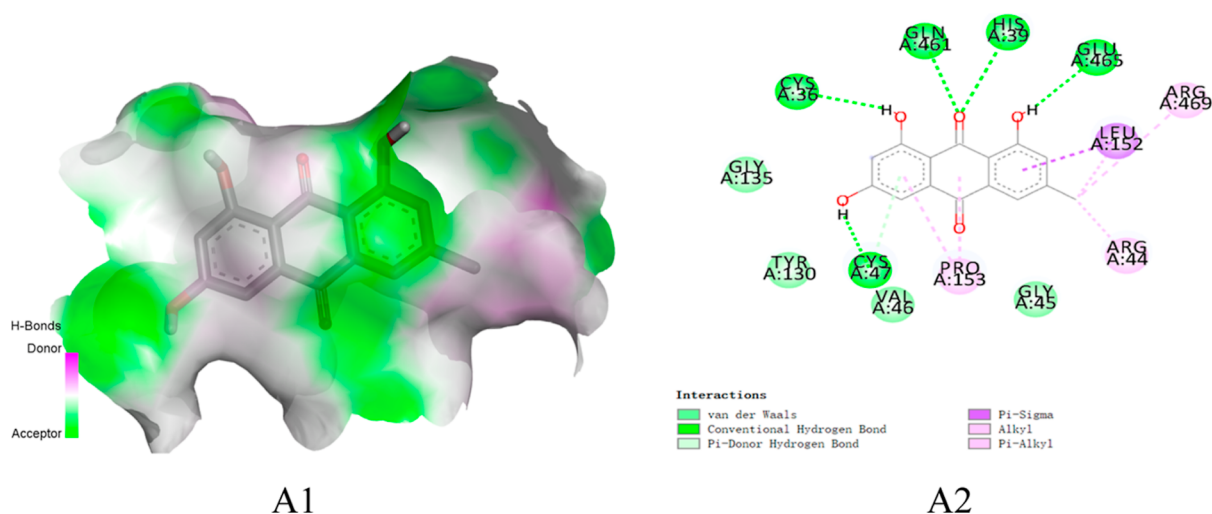


**Figure 8.** Schematic diagram of molecular docking between emodin and VEGF-A. A1 and A2 represent hydrogen bonding and 2D plan views, respectively. It can be seen from the 2D plane that there are many interactions between emodin and VEGF-A, such as hydrogen bond, van der Waals force, and  $\pi$  bond.

**Table 5. Docking Information of Emodin and Core Targets**

receptor	emodin		
	binding energy score (Gb/K cal/mol)	PDB ID	combining with the residue
VEGFA	-9.7	3QTK	TYR130, CYS47, HIS39, ARG469, ARG44, GLN461, LEU152, PRO153
PTGS2	-8.7	5F19	GLN203, HIS207, TYR385
TNF	-9.0	2E7A	GLN102, ARG98, SER99
CASP3	-8.1	3DEK	ARG164, GLY125, THR140, PRO201, TYR195
TP53	-7.0	4MZI	ARG158, THR256, SER99, ARG267

significant astrocyte aggregation in the VEGF-A immunostaining region. Emodin administration obviously reduces the number of double stained cells ( $P < 0.05$ ). The data indicated that emodin inhibited the activation of VEGF-A induced by astrocyte. In order to observe the effect of emodin on oxidative stress of neurons in MCAO rats, as shown in Figure 13b,d, we performed immunofluorescence and found that emodin decreased the level of Hif-1 $\alpha$  ( $P < 0.05$ ). The results suggest that emodin could inhibit the release of Hif-1 $\alpha$  from neurons after ischemia, thereby down-regulating the Hif-1 $\alpha$ /VEGF-A signal.

#### 4. DISCUSSION

Emodin, a natural compound with good anti-inflammatory, antioxidant, and vascular endothelial function regulation properties, is widely used in various inflammatory and tumor-related diseases.<sup>33</sup> Currently, many studies have confirmed that emodin has a certain effect on ischemic stroke,<sup>15–17</sup> but its action mechanism needs to be explored in depth. In this study, a combination of network pharmacology and animal experiments was used to explore the action mechanism of emodin in MCAO treatment. First, we observed that in the MCAO rat model, emodin improved the clinical symptoms of MCAO within 24 h and reduced their infarct volume. The results are consistent with those of previous reports, suggesting that emodin can reduce acute cerebral I/R injury and provide certain neuroprotective effects.

Next, we used network pharmacology to explore the potential targets of emodin in ischemic stroke treatment. The PPI network and drug–target–disease pathway network revealed that multiple interacting targets exist between emodin and ischemic stroke at the genetic and molecular levels. Among them, VEGF-A, TNF, caspase-3, TP53, and prostaglandin-endoperoxide synthase were the top 5 targets according to the PPI network. Furthermore, we conducted molecular docking to verify the aforementioned targets. The results showed that the bond between emodin and VEGF-A was the most stable according to the binding potency and hydrogen bonding. Hence, we speculated that emodin may have a therapeutic effect on ischemic stroke through VEGF-A regulation. Subsequent immunohistochemistry and immunoblotting results revealed that emodin down-regulated the expression of VEGF-A in MCAO. These findings have not been reported in previous trials of emodin treatment for MCAO. However, in multiple tumor-related studies, emodin has been reported to reduce microvascular proliferation and tissue inflammation through the inhibition of VEGF-A activation.<sup>34–36</sup> This enlightened us to analyze whether emodin is efficacious in the treatment of MCAO through a similar mechanism.

Ischemia reperfusion is crucial to improve the hypoxic state of ischemia. However, in the acute phase of ischemic stroke, reperfusion of the infarct area may lead to poor prognoses, such as the enlargement of infarct volume and aggravation of neurological symptoms, which may be caused by damage to the local BBB, oxidative stress, inflammation, and cellular edema.<sup>2,7,37</sup> VEGF can promote angiogenesis and increase vascular permeability. After cerebral ischemia, it can induce peripheral angiogenesis around the lesion, increase ischemia penumbra perfusion, and improve tissue blood supply.<sup>38</sup> However, the excessive activation of VEGF in the early stage increases the leakage of BBB, aggravates the oxidative stress and inflammatory injury of lesions, and causes brain edema, which in turn leads to the expansion of volume of infarction.<sup>5,39,40</sup> Zhang *et al.* found that exogenous administration of VEGF treatment 48 h after ischemia can increase angiogenesis in the ischemic penumbra of MCAO rats and significantly promotes the recovery of nerve function. However, early treatment after ischemia (after 1 h) increases the risk of BBB leakage,

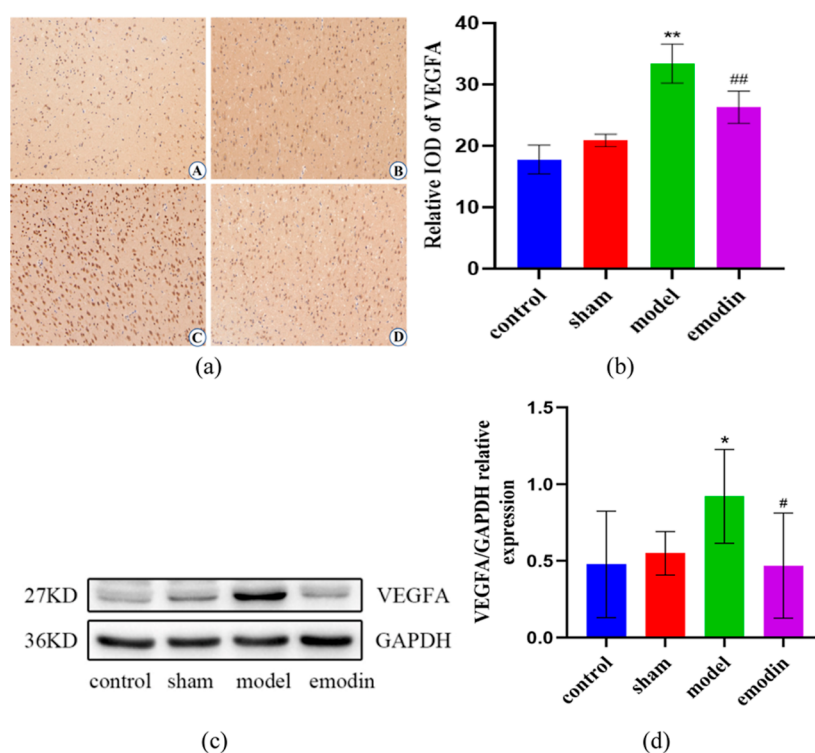


**Figure 9.** Effects of emodin on VEGF-A expression in MCAO rats. (a,b) are typical images and quantitative histograms of immunohistochemistry of VEGF-A, respectively. A, B, C, and D represent normal group, sham group, model group, and emodin group, respectively. (c,d) represent electrophoretic images and quantitative histogram of VEGF-A, respectively. Data are presented as mean  $\pm$  SEM; \* $P$  < 0.05, \*\* $P$  < 0.01 vs sham group; # $P$  < 0.05, ## $P$  < 0.01 vs model group.

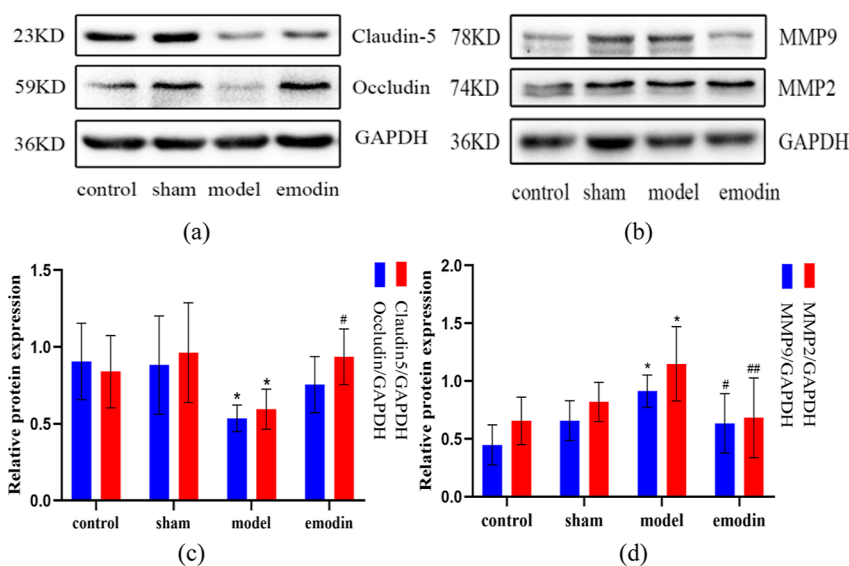


**Figure 10.** Effect of emodin on the expression of tight junction-related proteins and MMP-2/MMP-9 expression in the brain tissue of MCAO rats. (a,c) electrophoretic and statistical correlation histograms of occludin and claudin-5 proteins in brain tissue of rats in each group. (b,d) electrophoretic and statistical correlation histograms of MMP2 and MMP9 proteins in brain tissue of rats in each group. Data are presented as mean  $\pm$  SEM; \* $P$  < 0.05, \*\* $P$  < 0.01 vs sham group; # $P$  < 0.05, ## $P$  < 0.01 vs model group.

hemorrhagic transformation, and inflammatory damage.<sup>3</sup> Studies have shown that intravenous administration of VEGF 1 h after reperfusion increased infarct volume and BBB leakage in mice.<sup>5</sup> Therefore, some scholars believe that VEGF-A is unfavorable for disease prognosis in the early stage of stroke, especially within 24 h.<sup>41</sup> In our study, high levels of VEGF-A were associated with severe neurological scores and large infarct volumes, suggesting that VEGF-A is a potential target for

emodin in MCAO treatment. After cerebral ischemia and hypoxia, the I/R injury caused by VEGF-A is mainly achieved through the destruction of the BBB and activation of the inflammatory cascade.<sup>3</sup> VEGF-A activation can cause vascular endothelial dysfunction and induce the secretion of various pro-inflammatory factors (TNF- $\alpha$ , interleukin [IL]-1 $\beta$ , etc.) and matrix metalloprotein kinases (MMP-2/MMP-9, etc.), resulting in tight-junction (TJ) protein and transmembrane protein

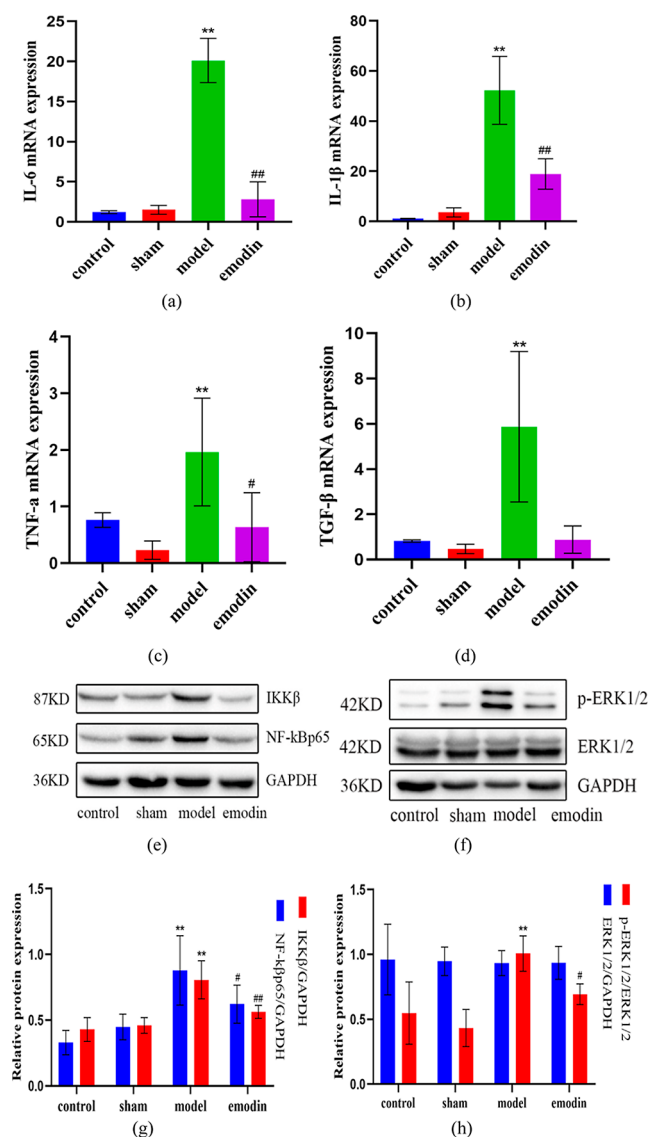


**Figure 11.** Effect of emodin on the expression of inflammatory factors mRNA in the brain tissue of MCAO model rats. (a–d) represent the mRNA expression of IL-6, IL-1 $\beta$ , TNF- $\alpha$ , and TGF- $\beta$ 1, respectively. (e–h) NF- $\kappa$ B and IKK $\beta$  protein electrophoresis and statistical histogram. Data are presented as mean  $\pm$  SEM; \* $P$  < 0.05, \*\* $P$  < 0.01 vs sham group; # $P$  < 0.05, ### $P$  < 0.01 vs model group.

degradation, increasing BBB permeability.<sup>28,42,43</sup> The opening of the BBB encourages peripheral immune cells (such as macrophages, neutrophils, *etc.*) to invade to the center, aggravating the oxidative stress and inflammatory response in the infarct area, resulting in cellular edema and necrosis in the infarct focus.<sup>43–45</sup> Therefore, inhibiting inflammation and protecting the BBB are key to the treatment of this disease. In our experiments, the degradation of occludin and claudin-5 proteins significantly reduced after emodin treatment, and furthermore, the protein expression levels of MMP-9 and MMP-2 reduced. Emodin may protect the BBB through the inhibition of TJ protein disruption caused by matrix metalloproteinases and the reduction of vascular leakage caused by an ischemic stroke.

Among TJ proteins constituting the BBB, claudin is the most important. In particular, the expression of claudin-5 in the BBB is approximately 100 times higher than that in other tissues.<sup>46</sup> It

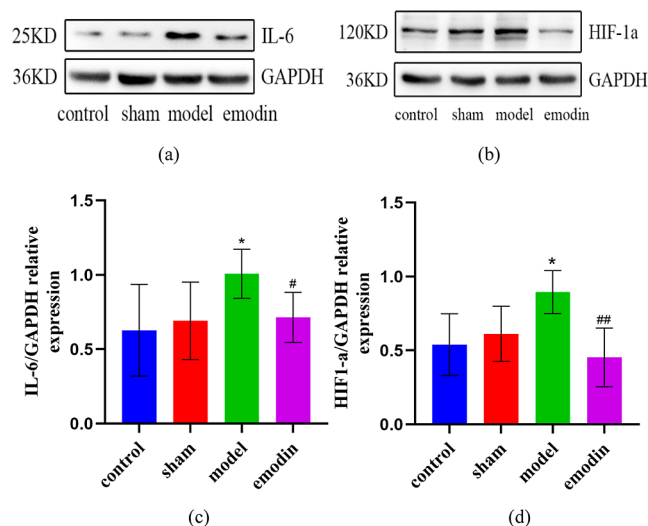


**Figure 12.** Protein expression levels of IL-6 and Hif-1 $\alpha$  in cerebral infarction tissues of rats in each group. (a,b) represent electrophoretic diagrams, and (c,d) represent bar diagrams for quantitative analysis. Data are presented as mean  $\pm$  SEM; \* $P$  < 0.05, \*\* $P$  < 0.01 vs sham group; # $P$  < 0.05, ### $P$  < 0.01 vs model group.

plays a crucial role in the formation and integrity of TJ proteins and determines the function of the barrier. Other proteins include the TJ-associated MARVEL protein family, such as occludin and tricellular TJs, and the zonula occludens (ZO) family of cytoplasmic proteins, including ZO-1. Studies have shown that occludin has no effect on the morphology of mouse TJ, but it weakens the localization of tricell protein, suggesting that tricell may compensate for part of the function of occludin.<sup>47</sup> Meanwhile, we noticed that emodin pre-treatment did not significantly increase the expression level of occludin compared with claudin-5 protein. It may be that emodin has a protective effect on the inherent components of BBB and prevents its degradation due to ischemia and hypoxia, because occludin tends to protect the barrier rather than assemble. However, the specific mechanism needs to be further clarified. On the other hand, we studied the expression of TJ-related proteins 24 h after ischemia-reperfusion. A study showed that the expression level of occludin decreased in hypoxia, but it had little effect on claudin-5, suggesting that it may be involved in oxygen recovery during reperfusion in rats.<sup>28</sup> However, a study demonstrated that rats treated with 6% oxygen for 1 h and subjected to reoxygenation for 10 min showed no significant difference in the expression level of occludin compared with controls, except that the phosphorylation level of occludin changed. These studies have suggested that strong fluctuations in occludin may be related to the oxygen level, but further experiments are needed to explore this relationship, including the phosphorylation of occludin, time of ischemia and reperfusion, and expression of the tricellular protein.

VEGF-A can activate downstream inflammation and cell proliferation signals through ERK and nuclear factor kappa B (NF- $\kappa$ B). As a multifunctional nuclear factor, NF- $\kappa$ B forms a complex signal network with various proteins in the cytoplasm and participates in the activation and amplification of various inflammations.<sup>30</sup> Among them, mitogen-activated protein kinase delivers various pro-inflammatory substances to the nucleus and regulates gene expression through NF- $\kappa$ B. In the MCAO model, knocking out the NF- $\kappa$ B gene or ligand can alleviate the symptoms of MCAO.<sup>48</sup> Inhibition of the ERK1/2

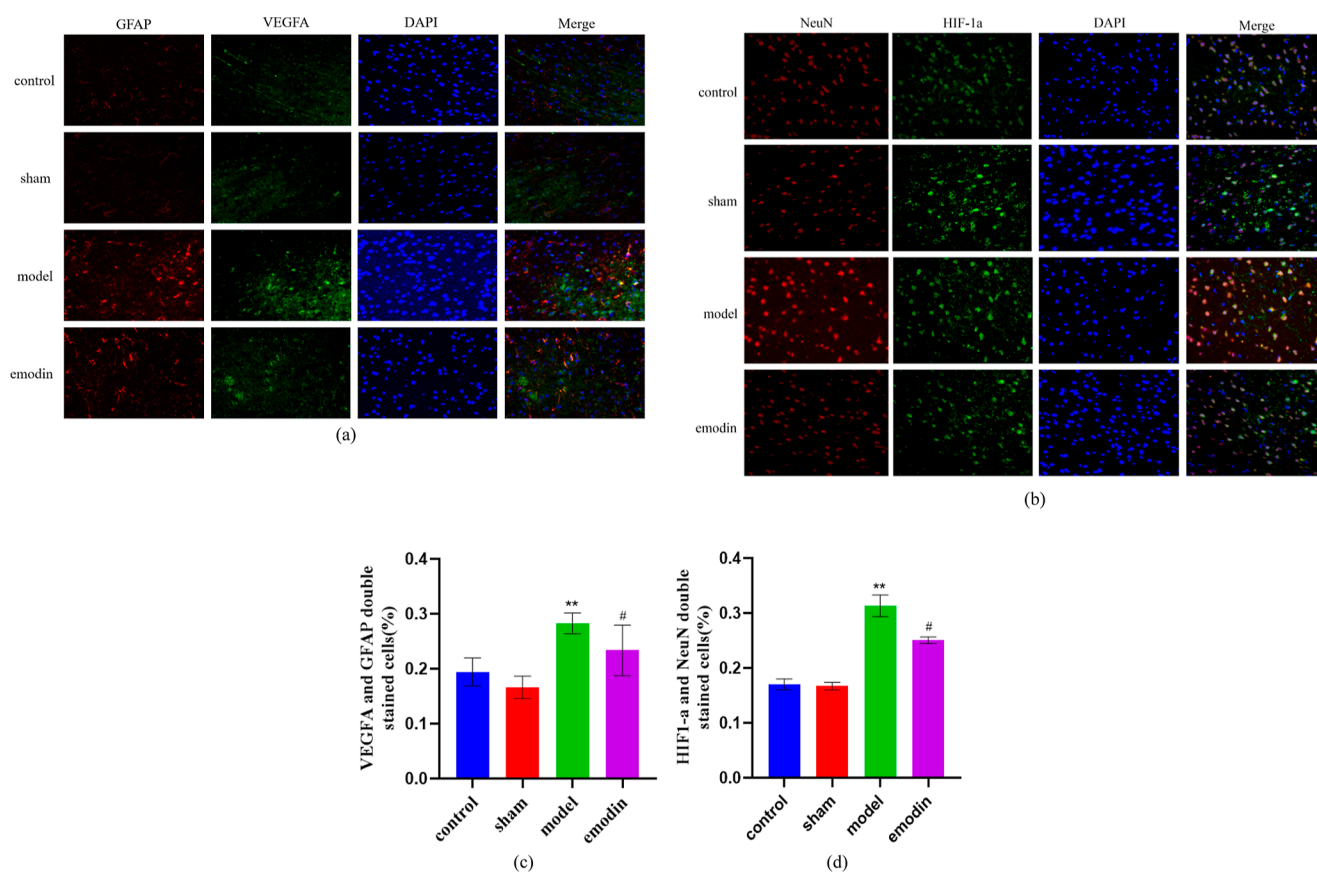


**Figure 13.** Immunofluorescence images and quantitative analysis of VEGF-A and Hif-1 $\alpha$ . (a,c) VEGF-A and GFAP fluorescence double co-localization and the relevant quantitative analysis. VEGF-A (green), GFAP (red), and DAPI (nuclei marker, blue). (b,d) Hif-1 $\alpha$  and NeuN fluorescence double co-localization and the relevant quantitative analysis (200 $\times$ ). Data are presented as mean  $\pm$  SEM; \* $P$  < 0.05, \*\* $P$  < 0.01 vs sham group; # $P$  < 0.05, ## $P$  < 0.01 vs model group.

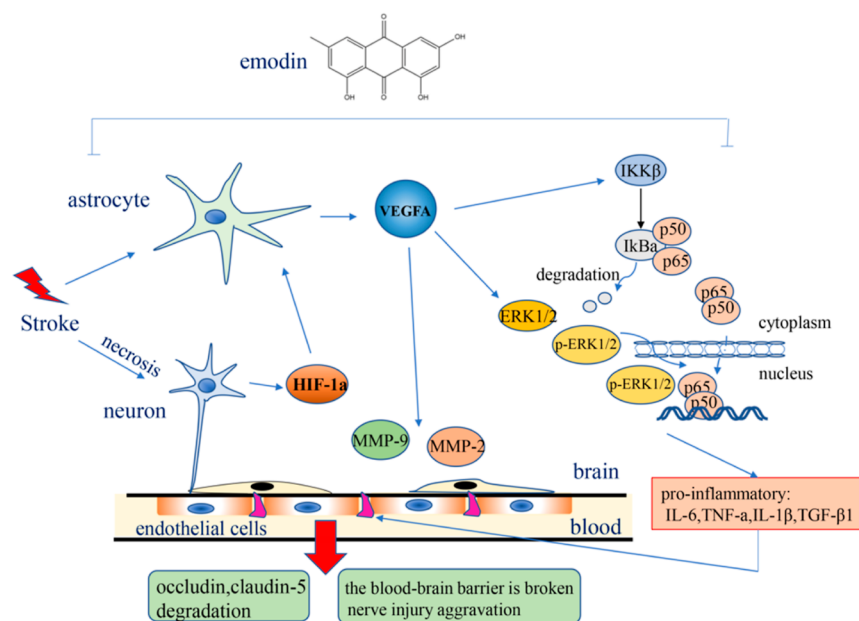


**Figure 14.** The release of Hif-1 $\alpha$  after neuronal necrosis induces the expression of VEGF-A in astrocytes, which plays an important role in the mechanism of inflammatory injury in the early stage of ischemic stroke. Emodin may reduce the BBB leakage and the inflammatory response caused by ERK/IKK $\beta$ /NF- $\kappa$ B activation by inhibiting Hif-1 $\alpha$ /VEGF-A signal, so as to improve the early injury of ischemic stroke.

pathway can reduce the expression of pro-inflammatory cytokines such as IL-6, TNF-A, TGF- $\beta$ , and IL-1 $\beta$  and protect the infarct site.<sup>44</sup> In our experiments, emodin inhibited the

activation of the ERK/IKK beta/NF- $\kappa$ B pathway and at the same time significantly down-regulated the mRNA transcription levels of downstream cytokines IL-6, TNF-a, TGF- $\beta$ , and IL-1 $\beta$ .

The accumulation of these inflammatory factors stimulates the activation of glial cells in the brain and aggravates cytotoxic damage.<sup>49</sup> Under ischemia and hypoxia, the brain's innate immune cells, astrocytes, proliferate reactively, accompanied by the expression of the GFAP and the secretion of numerous inflammatory factors such as IL-6.<sup>38,40</sup> Necrotic neurons can release hypoxia-inducible factor (Hif)-1 $\alpha$ , induce astrocytes to express VEGF-A, cause inflammation in the infarct area, and aggravate BBB destruction and neuronal necrosis.<sup>32</sup>

In ischemic stroke, Hif-1 $\alpha$  is involved in the upregulation of pro-inflammatory chemokines and cytokines in epithelial cells through the NF- $\kappa$ B pathway.<sup>45</sup> Simultaneously, it is also involved in the metabolism and signal transduction of astrocytes in response to oxidative stress.<sup>50</sup> First, we used WB to detect the protein expression levels of Hif-1 $\alpha$  and IL-6 and found that emodin can reduce the expression of Hif-1 $\alpha$  and IL-6, markers of inflammatory damage. Subsequently, we used immunofluorescence double labeling to detect Hif-1 $\alpha$ (+)-NeuN(+) cells and VEGF(+)-GFAP(+) cells. The results showed that the expression of the aforementioned two markers in the model group increased significantly, whereas that in the emodin group decreased significantly. Emodin may reduce the inflammatory injury of infarcted tissue through the reduction of Hif-1 $\alpha$  release from neurons and inhibition of VEGF-A overexpression induced by astrocytes.

## 5. CONCLUSIONS

In summary, our study is the first to demonstrate the efficacy of emodin in the treatment of ischemic stroke within 24 h. Subsequently, network pharmacology and molecular docking revealed that VEGF-A is the key target of emodin in ischemic stroke treatment. Through a quantitative reverse-transcription polymerase chain reaction, WB, immunofluorescence, immunohistochemistry, and other techniques, we found that emodin may reduce the expression of Hif-1 $\alpha$ , inhibit the secretion of VEGF-A derived from astrocytes, and down-regulate ERK/inhibitor of NF- $\kappa$ B kinase/NF- $\kappa$ B inflammation signals, thereby reducing the damage of the BBB and infarct site (Figure 14). Our experimental results show that emodin has the effects of anti-inflammation, antioxidation, and vascular endothelial function regulation, which provides an experimental basis for the treatment of ischemic stroke with traditional Chinese medicine. However, the mechanisms of I/R injury are complex, as described in previous studies. VEGF-A has a positive effect on the improvement of blood supply to the brain, angiogenesis promotion, and tissue repair after 48 h of stroke onset. Whether the inhibitory effect of emodin on VEGF-A affects angiogenesis and tissue repair in the later stage of ischemic stroke and whether it can reduce stroke severity for a long period after the onset is unknown. Therefore, further in-depth experiments on this topic are needed.

## AUTHOR INFORMATION

### Corresponding Authors

**Yuanqi Zhao** – Department of Encephalopathy, The Second Affiliated Hospital of Guangzhou University of Chinese Medicine, Guangzhou 510120, China; Email: [tcm2008@126.com](mailto:tcm2008@126.com)

**Zequan Zheng** – Department of Encephalopathy, The Second Affiliated Hospital of Guangzhou University of Chinese Medicine, Guangzhou 510120, China; Guangdong Provincial Hospital of Traditional Chinese Medicine, Guangzhou 510120, China; Doctor of equivalent degree, Guangzhou

University of Chinese Medicine, Guangzhou 510405, China; Email: [657950995@qq.com](mailto:657950995@qq.com)

### Authors

**Baojiang Lv** – The First Clinical Medical College, Guangzhou University of Chinese Medicine, Guangzhou 510405, China; Lingnan Medical Research Center, Guangzhou University of Chinese Medicine, Guangzhou 510405, China; [orcid.org/0000-0001-6054-2387](https://orcid.org/0000-0001-6054-2387)

**Kenan Zheng** – The First Clinical Medical College, Guangzhou University of Chinese Medicine, Guangzhou 510405, China; Lingnan Medical Research Center, Guangzhou University of Chinese Medicine, Guangzhou 510405, China

**Yifan Sun** – Department of Encephalopathy, The Second Affiliated Hospital of Guangzhou University of Chinese Medicine, Guangzhou 510120, China; Guangdong Provincial Hospital of Traditional Chinese Medicine, Guangzhou 510120, China

**Lulu Wu** – The First Clinical Medical College, Guangzhou University of Chinese Medicine, Guangzhou 510405, China; Lingnan Medical Research Center, Guangzhou University of Chinese Medicine, Guangzhou 510405, China

**Lijun Qiao** – Department of Encephalopathy, The Second Affiliated Hospital of Guangzhou University of Chinese Medicine, Guangzhou 510120, China

**Zhibing Wu** – Department of Encephalopathy, The First Affiliated Hospital of Guangzhou University of Chinese Medicine, Guangzhou 510405, China

Complete contact information is available at:

<https://pubs.acs.org/10.1021/acsomega.2c01897>

### Author Contributions

<sup>†</sup>B.L. and Y.S. contributed equally to this work.

### Author Contributions

Z.Z. and B.L. designed the experiment and composed the manuscript. B.L. and K.Z. conducted animal experiments. B.L., Y.S., and K.Z. carried out the experimental detection. B.L., Y.S., K.Z., and L.W. performed statistics and graphed the data. M.Z. modified the language of the whole article. Y.Z., L.Q., and Z.W. provided funding to support the study. Z.Z. reviewed the final manuscript. All authors have read and agreed to the published version of the manuscript.

### Notes

The authors declare no competing financial interest.

The authors have completed the MDAR reporting checklist. The authors are accountable for all aspects of the work in ensuring that questions related to the accuracy or integrity of any part of the work are appropriately investigated and resolved.

## ACKNOWLEDGMENTS

We sincerely thank Lingnan Medical Center of Guangzhou University of Chinese Medicine for providing the laboratory facilities and equipment. This research was supported by the Special Project of Guangdong Provincial Key Laboratory of Traditional Chinese Medicine Emergency Research (no.: 2019KT1340) and the Natural Science Foundation of Guangdong Province (no.: 2018A0303130053).

## REFERENCES

- (1) Wu, S.; Wu, B.; Liu, M.; Chen, Z.; Wang, W.; Anderson, C. S.; Sandercock, P.; Wang, Y.; Huang, Y.; Cui, L.; Pu, C.; Jia, J.; Zhang, T.; Liu, X.; Zhang, S.; Xie, P.; Fan, D.; Ji, X.; Wong, K.-S. L.; Wang, L.; Wu, S.; Wu, B.; Liu, M.; Chen, Z.; Wang, W.; Anderson, C. S.; Sandercock,

- P.; Wang, Y.; Huang, Y.; Cui, L.; Pu, C.; Jia, J.; Zhang, T.; Liu, X.; Zhang, S.; Xie, P.; Fan, D.; Ji, X.; Wong, K.-S. L.; Wang, L.; Wei, C.; Wang, Y.; Cheng, Y.; Liu, Y.; Li, X.; Dong, Q.; Zeng, J.; Peng, B.; Xu, Y.; Yang, Y.; Wang, Y.; Zhao, G.; Wang, W.; Xu, Y.; Yang, Q.; He, Z.; Wang, S.; You, C.; Gao, Y.; Zhou, D.; He, L.; Li, Z.; Yang, J.; Lei, C.; Zhao, Y.; Liu, J.; Zhang, S.; Tao, W.; Hao, Z.; Wang, D.; Zhang, S. China Stroke Study Collaboration. Stroke in China: advances and challenges in epidemiology, prevention, and management. *Lancet Neurol.* **2019**, *18*, 394–405.
- (2) Jayaraj, R. L.; Azimullah, S.; Beiram, R.; Jalal, F. Y.; Rosenberg, G. A. Neuroinflammation: friend and foe for ischemic stroke. *J. Neuroinflammation* **2019**, *16*, 142.
- (3) Zhang, Z. G.; Zhang, L.; Jiang, Q.; Zhang, R.; Davies, K.; Powers, C.; Bruggen, N. V.; Chopp, M. VEGF enhances angiogenesis and promotes blood-brain barrier leakage in the ischemic brain. *J. Clin. Invest.* **2000**, *106*, 829–838.
- (4) Kaya, D.; Gürsoy-Özdemir, Y.; Yemisci, M.; Tuncer, N.; Aktan, S.; Dalkara, T. VEGF protects brain against focal ischemia without increasing blood-brain permeability when administered intracerebroventricularly. *J. Cereb. Blood Flow Metab.* **2005**, *25*, 1111–1118.
- (5) Geiseler, S. J.; Morland, C. The Janus Face of VEGF in Stroke. *Int. J. Mol. Sci.* **2018**, *19*, 1362.
- (6) Fukuta, T.; Asai, T.; Yanagida, Y.; Namba, M.; Koide, H.; Shimizu, K.; Oku, N. Combination therapy with liposomal neuroprotectants and tissue plasminogen activator for treatment of ischemic stroke. *FASEB J.* **2017**, *31*, 1879–1890.
- (7) Khatri, R.; McKinney, A. M.; Swenson, B.; Janardhan, V. Blood-brain barrier, reperfusion injury, and hemorrhagic transformation in acute ischemic stroke. *Neurology* **2012**, *79*, S52–S57.
- (8) Wang, X. D.; Su, G. Y.; Zhao, C.; Qu, F. Z.; Wang, P.; Zhao, Y. Q. Anticancer activity and potential mechanisms of 1C, a ginseng saponin derivative, on prostate cancer cells. *J. Ginseng Res.* **2018**, *42*, 133–143.
- (9) Han, Q.; Tang, H.-z.; Zou, M.; Zhao, J.; Wang, L.; Bian, Z.-x.; Li, Y.-h. Anti-inflammatory Efficacy of Combined Natural Alkaloid Berberine and S1PR Modulator Fingolimod at Low Doses in Ulcerative Colitis Preclinical Models. *J. Nat. Prod.* **2020**, *83*, 1939–1949.
- (10) Bagherniya, M.; Darand, M.; Askari, G.; Guest, P. C.; Sathyapalan, T.; Sahebkar, A. The Clinical Use of Curcumin for the Treatment of Rheumatoid Arthritis: A Systematic Review of Clinical Trials. *Adv. Exp. Med. Biol.* **2021**, *1291*, 251–263.
- (11) Zhang, L.; Liu, H.; Qin, L.; Zhang, Z.; Wang, Q.; Zhang, Q.; Lu, Z.; Wei, S.; Gao, X.; Tu, P. Global chemical profiling based quality evaluation approach of rhubarb using ultra performance liquid chromatography with tandem quadrupole time-of-flight mass spectrometry. *J. Sep. Sci.* **2015**, *38*, 511–522.
- (12) Liu, J.; Li, G.; Chen, Y.-z.; Zhang, L.-d.; Wang, T.; Wen, Z.-l.; Wang, L.; Chen, D.-c. Effects of rhubarb on the expression of glucocorticoids receptor and regulation of cellular immunity in burn-induced septic rats. *Chin. Med. J.* **2019**, *132*, 1188–1193.
- (13) Shia, C.-s.; Suresh, G.; Hou, Y.-c.; Lin, Y.-c.; Chao, P.-D. L.; Juang, S.-H. Suppression on metastasis by rhubarb through modulation on MMP-2 and uPA in human A549 lung adenocarcinoma: an ex vivo approach. *J. Ethnopharmacol.* **2011**, *133*, 426–433.
- (14) Tsai, K.-H.; Hsien, H.-H.; Chen, L.-m.; Ting, W.-j.; Yang, Y.-s.; Kuo, C.-h.; Tsai, C.-H.; Tsai, F.-J.; Tsai, H. J.; Huang, C.-y. Rhubarb inhibits hepatocellular carcinoma cell metastasis via GSK-3 $\beta$  activation to enhance protein degradation and attenuate nuclear translocation of  $\beta$ -catenin. *Food Chem.* **2013**, *138*, 278–285.
- (15) Li, Y.; Xu, Q.-q.; Shan, C.-s.; Shi, Y.-h.; Wang, Y.; Zheng, G.-q. Combined Use of Emodin and Ginsenoside Rb1 Exerts Synergistic Neuroprotection in Cerebral Ischemia/Reperfusion Rats. *Front. Pharmacol.* **2018**, *9*, 943.
- (16) Leung, S. W.; Lai, J. H.; Wu, J. C.-C.; Tsai, Y.-R.; Chen, Y.-h.; Kang, S.-J.; Chiang, Y.-H.; Chang, C.-f.; Chen, K.-y. Neuroprotective Effects of Emodin against Ischemia/Reperfusion Injury through Activating ERK-1/2 Signaling Pathway. *Int. J. Mol. Sci.* **2020**, *21*, 2899.
- (17) Xian, M.; Cai, J.; Zheng, K.; Liu, Q.; Liu, Y.; Lin, H.; Liang, S.; Wang, S. Aloe-emodin prevents nerve injury and neuroinflammation caused by ischemic stroke via the PI3K/AKT/mTOR and NF- $\kappa$ B pathway. *Food Funct.* **2021**, *12*, 8056–8067.
- (18) Cui, Y.; Chen, L.-j.; Huang, T.; Ying, J.-q.; Li, J. The pharmacology, toxicology and therapeutic potential of anthraquinone derivative emodin. *Chin. J. Nat. Med.* **2020**, *18*, 425–435.
- (19) Gfeller, D.; Grosdidier, A.; Wirth, M.; Daina, A.; Michielin, O.; Zoete, V. SwissTargetPrediction: a web server for target prediction of bioactive small molecules. *Nucleic Acids Res.* **2014**, *42*, W32–W38.
- (20) Xu, H.-Y.; Zhang, Y.-q.; Liu, Z.-m.; Chen, T.; Lv, C.-y.; Tang, S.-H.; Zhang, X.-b.; Zhang, W.; Li, Z.-y.; Zhou, R.-r.; Yang, H.-J.; Wang, X.-j.; Huang, L.-q. ETCM: an encyclopaedia of traditional Chinese medicine. *Nucleic Acids Res.* **2019**, *47*, D976–D982.
- (21) Kuhn, M.; von Mering, C.; Campillos, M.; Jensen, L. J.; Bork, P. STITCH: interaction networks of chemicals and proteins. *Nucleic Acids Res.* **2008**, *36*, D684–688.
- (22) Piñero, J.; Bravo, A.; Queralt-Rosinach, N.; Gutiérrez-Sacristán, A.; Deu-Pons, J.; Centeno, E.; García-García, J.; Sanz, F.; Furlong, L. I. DisGeNET: a comprehensive platform integrating information on human disease-associated genes and variants. *Nucleic Acids Res.* **2017**, *45*, D833–D839.
- (23) Rebhan, M.; Chalifa-Caspi, V.; Prilusky, J.; Lancet, D. GeneCards: integrating information about genes, proteins and diseases. *Trends Genet.* **1997**, *13*, 163.
- (24) Guo, P.; Jin, Z.; Wu, H.; Li, X.; Ke, J.; Zhang, Z.; Zhao, Q. Effects of irisin on the dysfunction of blood-brain barrier in rats after focal cerebral ischemia/reperfusion. *Brain Behav.* **2019**, *9*, No. e01425.
- (25) Lu, J.; Wang, J.; Yu, L.; Cui, R.; Zhang, Y.; Ding, H.; Yan, G. Treadmill Exercise Attenuates Cerebral Ischemia-Reperfusion Injury by Promoting Activation of M2 Microglia via Upregulation of Interleukin-4. *Front. Cardiovasc. Med.* **2021**, *8*, 735485.
- (26) Zheng, K.; Lv, B.; Wu, L.; Wang, C.; Xu, H.; Li, X.; Wu, Z.; Zhao, Y.; Zheng, Z. Protecting effect of emodin in experimental autoimmune encephalomyelitis mice by inhibiting microglia activation and inflammation via Myd88/PI3K/Akt/NF- $\kappa$ B signalling pathway. *Bioengineering* **2022**, *13*, 9322–9344.
- (27) Kong, Y.; Ma, X.; Zhang, X.; Wu, L.; Chen, D.; Su, B.; Liu, D.; Wang, X. The potential mechanism of Fructus Ligustri Lucidi promoting osteogenic differentiation of bone marrow mesenchymal stem cells based on network pharmacology, molecular docking and experimental identification. *Bioengineered* **2022**, *13*, 10640–10653.
- (28) Bauer, A. T.; Bürgers, H. F.; Rabie, T.; Marti, H. H. Matrix metalloproteinase-9 mediates hypoxia-induced vascular leakage in the brain via tight junction rearrangement. *J. Cereb. Blood Flow Metab.* **2010**, *30*, 837–848.
- (29) Sasaki, R.; Yamashita, T.; Tadokoro, K.; Matsumoto, N.; Nomura, E.; Omote, Y.; Takemoto, M.; Hishikawa, N.; Ohta, Y.; Abe, K. Direct arterial damage and neurovascular unit disruption by mechanical thrombectomy in a rat stroke model. *J. Neurosci. Res.* **2020**, *98*, 2018–2026.
- (30) Marumo, T.; Schini-Kerth, V. B.; Busse, R. Vascular endothelial growth factor activates nuclear factor-kappaB and induces monocyte chemoattractant protein-1 in bovine retinal endothelial cells. *Diabetes* **1999**, *48*, 1131–1137.
- (31) Li, Y.-n.; Pan, R.; Qin, X.-J.; Yang, W.-l.; Qi, Z.; Liu, W.; Liu, K. J. Ischemic neurons activate astrocytes to disrupt endothelial barrier via increasing VEGF expression. *J. Neurochem.* **2014**, *129*, 120–129.
- (32) Rattner, A.; Williams, J.; Nathans, J. Roles of HIFs and VEGF in angiogenesis in the retina and brain. *J. Clin. Invest.* **2019**, *129*, 3807–3820.
- (33) Shrimali, D.; Shanmugam, M. K.; Kumar, A. P.; Zhang, J.; Tan, B. K. H.; Ahn, K. S.; Sethi, G. Targeted abrogation of diverse signal transduction cascades by emodin for the treatment of inflammatory disorders and cancer. *Cancer Lett.* **2013**, *341*, 139–149.
- (34) Kwak, H.-J.; Park, M.-J.; Park, C.-M.; Moon, S.-I.; Yoo, D.-H.; Lee, H.-C.; Lee, S.-H.; Kim, M.-S.; Lee, H.-W.; Shin, W.-S.; Park, I.-C.; Rhee, C. H.; Hong, S.-I. Emodin inhibits vascular endothelial growth factor-A-induced angiogenesis by blocking receptor-2 (KDR/Flk-1) phosphorylation. *Int. J. Cancer* **2006**, *118*, 2711–2720.

- (35) Wu, J.; Ke, X.; Wang, W.; Zhang, H.; Ma, N.; Fu, W.; Zhao, M.; Gao, X.; Hao, X.; Zhang, Z. Aloe-emodin suppresses hypoxia-induced retinal angiogenesis via inhibition of HIF-1 $\alpha$ /VEGF pathway. *Int. J. Biol. Sci.* **2016**, *12*, 1363–1371.
- (36) Zou, G.; Zhang, X.; Wang, L.; Li, X.; Xie, T.; Zhao, J.; Yan, J.; Wang, L.; Ye, H.; Jiao, S.; Xiang, R.; Shi, Y. Herb-sourced emodin inhibits angiogenesis of breast cancer by targeting VEGFA transcription. *Theranostics* **2020**, *10*, 6839–6853.
- (37) Eltzschig, H. K.; Eckle, T. Ischemia and reperfusion—from mechanism to translation. *Nat. Med.* **2011**, *17*, 1391–1401.
- (38) Gu, W.; Brännström, T.; Jiang, W.; Bergh, A.; Wester, P. Vascular endothelial growth factor-A and -C protein up-regulation and early angiogenesis in a rat photothrombotic ring stroke model with spontaneous reperfusion. *Acta Neuropathol.* **2001**, *102*, 216–226.
- (39) Obermeier, B.; Daneman, R.; Ransohoff, R. M. Development, maintenance and disruption of the blood-brain barrier. *Nat. Med.* **2013**, *19*, 1584–1596.
- (40) Yang, C.; Hawkins, K. E.; Doré, S.; Candelario-Jalil, E. Neuroinflammatory mechanisms of blood-brain barrier damage in ischemic stroke. *Am. J. Physiol. Cell Physiol.* **2019**, *316*, C135–C153.
- (41) Weis, S. M.; Cheres, D. A. Pathophysiological consequences of VEGF-induced vascular permeability. *Nature* **2005**, *437*, 497–504.
- (42) Valable, S.; Montaner, J.; Bellail, A.; Berezowski, V.; Brillault, J.; Cecchelli, R.; Divoux, D.; Mackenzie, E. T.; Bernaudin, M.; Rousset, S.; Petit, E. VEGF-induced BBB permeability is associated with an MMP-9 activity increase in cerebral ischemia: both effects decreased by Ang-1. *J. Cereb. Blood Flow Metab.* **2005**, *25*, 1491–1504.
- (43) Lasek-Bal, A.; Jedrzejowska-Szypulka, H.; Student, S.; Warszwiancka, A.; Zareba, K.; Puz, P.; Bal, W.; Pawletko, K.; Lewin-Kowalik, J. The importance of selected markers of inflammation and blood-brain barrier damage for short-term ischemic stroke prognosis. *J. Physiol. Pharmacol.* **2019**, *70*, 209.
- (44) Jian, Z.; Liu, R.; Zhu, X.; Smerin, D.; Zhong, Y.; Gu, L.; Fang, W.; Xiong, X. The Involvement and Therapy Target of Immune Cells After Ischemic Stroke. *Front. Immunol.* **2019**, *10*, 2167.
- (45) Orellana-Urzúa, S.; Rojas, I.; Líbano, L.; Rodrigo, R. Pathophysiology of Ischemic Stroke: Role of Oxidative Stress. *Curr. Pharm. Des.* **2020**, *26*, 4246–4260.
- (46) Haseloff, R. F.; Dithmer, S.; Winkler, L.; Wolburg, H.; Blasig, I. E. Transmembrane proteins of the tight junctions at the blood-brain barrier: structural and functional aspects. *Semin. Cell Dev. Biol.* **2015**, *38*, 16–25.
- (47) Ikenouchi, J.; Sasaki, H.; Tsukita, S.; Furuse, M.; Tsukita, S. Loss of occludin affects tricellular localization of tricellulin. *Mol. Biol. Cell* **2008**, *19*, 4687–4693.
- (48) Schneider, A.; Martin-Villalba, A.; Weih, F.; Vogel, J.; Wirth, T.; Schwaninger, M. NF- $\kappa$ B is activated and promotes cell death in focal cerebral ischemia. *Nat. Med.* **1999**, *5*, 554–559.
- (49) Xu, S.; Lu, J.; Shao, A.; Zhang, J. H.; Zhang, J. Glial Cells: Role of the Immune Response in Ischemic Stroke. *Front. Immunol.* **2020**, *11*, 294.
- (50) Rossi, D. J.; Brady, J. D.; Mohr, C. Astrocyte metabolism and signaling during brain ischemia. *Nat. Neurosci.* **2007**, *10*, 1377–1386.